Materials Science Forum Vols. 633-634 (2010) pp 321-332
Online available since 2009/Nov/19 at www.scientific.net

doi:10.4028/www.scientific.net/MSF.633-634.321

Enhanced Ductility in Ultrafine-Grained Al Alloys Produced by SPD Techniques

Ruslan Z. Valiev[1,a,*], Maxim Yu. Murashkin[1,b], Boris B. Straumal[2,3,c]

[1]Institute of Physics of Advanced Materials, Ufa State Aviation Technical University
12 K. Marx str., Ufa 450000 Russia

[2]Institute of Solid State Physics, Russian Academy of Sciences, Chernogolovka, Moscow disctrict, 142432 Russia

[3]Max-Plank-Institute für Metallforschung, Heisenbergstrasse 3, 70569 Stuttgart, Germany

[a]rzvaliev@mail.rb.ru, [b]maxmur@mail.rb.ru, [c]straumal@issp.ac.ru

Keywords: ultrafine-grained structure, severe plastic deformation, equal channel angular pressing with parallel channels, high pressure torsion, strength and ductility.

Abstract. In this work ultrafine-grained (UFG) structure was successfully produced in the commercial Al 6061 and Al-30%Zn alloys using new modifications of two severe plastic deformation (SPD) techniques, namely equal channel angular pressing (ECAP) with parallel channels (PC) and high pressure torsion (HPT) with enhanced load. Variation of SPD processing regimes made it possible not only to perform strong grain refinement but also to modify the phase composition through the formation of grain boundary (GB) segregations and precipitations. This enabled to achieve a unique combination of high strength and ductility in the Al 6061 alloy and demonstrate super-ductility in the Al-30%Zn alloy, when elongation to failure exceeded 150% at room temperature.

Introduction

Fabrication of ultrafine-grained (UFG) metals and alloys by SPD processing has become a well-known direction in modern materials science [1-4]. These works started in the early 90-s with two techniques: equal channel angular pressing (ECAP) and high pressure torsion (HPT) [5], have been developed intensively last decade in connection with creation of principles of materials nanostructuring for advanced properties and elaboration of more effective SPD techniques [6]. Concerning mechanical properties [4,6], SPD drastically increases the strength of metals and alloys by decreasing their grain size into nanometer region. However, the ductility of such materials remains typically low. Therefore, to ensure simultaneously the high strength and high ductility of nanostructured metals is an important challenge for their advanced structural application. To date, a number of procedures and strategies were suggested to enhance ductility of nanostructured metals by keeping high strength. These approaches apply the formation of bimodal structures [7], introduction of second phases or twin boundaries into the nanostructured matrix [8] and GB engineering [9,10], i.e. control of UFG materials properties through tailoring specific interfaces by variation of SPD processing regimes and routes. In this work we succeeded to increase the room-temperature ductility of the SPD-processed Al-based alloys using this approach of GB engineering applying new modifications of two SPD techniques, namely ECAP-PC [6,11], and HPT with enhanced load [12].

Experimental Procedure

The investigations were conducted on two Al alloys – Al 6061 and Al-30%Zn. A commercial 6061 aluminum alloy (0.80Mg-0.41Si-0.12Cu-0.03Mn-0.02Ti-0.22Fe-balance Al (wt.%)) was used

* Corresponding Author, Email: RZValiev@mail.rb.ru

in a cast condition. The alloy under investigation was characterized by lower level of alloying elements (Si and Mg), comparing to traditional Al 6061 alloy [13]. Before SPD treatment, initial samples were subjected to solid solution treatment for 5 hours at 530°C with the following water quenching.

The Al-based alloy with 30 wt.% Zn was used after homogenization annealing, the microstructure contained equiaxial solid solution grains with a mean size about 65 μm.

The principles of ECAP PC are shown in Fig. 1 [6,11]. A distinctive feature of the ECAP-PC is that during a single processing pass, two distinct shearing events take place: shear in two deformation zones subsequently corresponding to two subsequent channels intersections in the die-set (Fig.1 a,b).

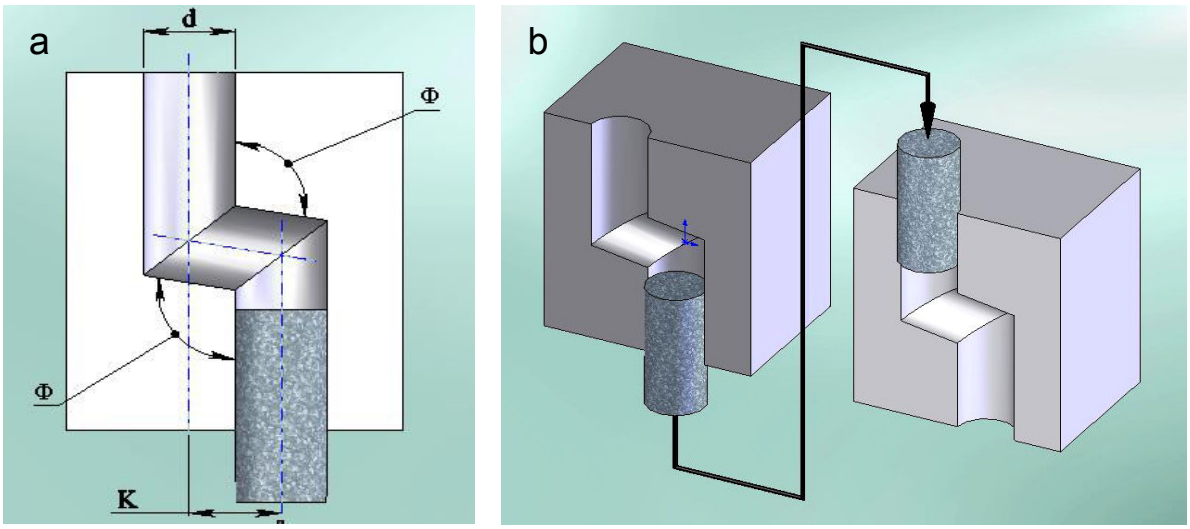

Fig. 1. The principles of ECAP-PC: d – diameter of the channel; K – is the distance between the axes of parallel channels; Φ – is the angle of intersection between the parallel channels and the channel joining them (a), route of 6061 alloy sample processing by ECAP-PC method (b).

The value of the displacement between the two channels, K, and the angle of intersection of the two channels Φ, are the main parameters of the die geometry, which influence both the flow pattern and the strain-stress state of the ECAP process. It has been established by computer simulation, that the optimal value of these parameters leading to the largest strain homogeneity are Φ = 100º and K = d, where d is the channel diameter [11]. Under these conditions, the accumulate strain for one pass is approximately equal to 2. The simulation results have been confirmed experimentally using a grid method. Furthermore, the studies showed that the deformation pattern realized in ECAP-PC die-set optimal geometry makes the structure homogeneous along the length of the bulk sample including up to the ends (the material utilization ratio is higher than 90 %).

Rods of 6061 Al alloy with the diameter of 18 mm and 100 mm length were subjected to ECAP-PC at 100°C, since the temperature provides significant grain refinement, preserving the facility for its further strengthening by subsequent aging at 160-175°C.

Vickers hardness (HV) was measured using a Micromet -5101 microidentation tester with a load of 200g for 15 s. In order to receive reliable results, each sample was measured more than 10 times.

Tensile tests at room temperature were performed on Instron 1185 at a strain rate of 5 x 10^{-4} s^{-1}. Mechanical properties were measured by at least 2 specimens with gage length 15 mm and diameter of 3 mm. Tensile specimens were cut of parallel to the longitudinal axis of the ECAP-processed material.

The structural characterization by TEM was performed in JEM-100B and JEOL-2000 EX electron microscopes using dark and bright fields. Average grain size was estimated from more than 250 grains measurement.

As for the Al-30%Zn alloy, after SPD processing by high pressure torsion the Al-based solid solution completely dissolved (XRD-spectra contained only the peaks of pure Al and Zn) [14]. The alloy was prepared of high purity components (5N5 Al and 5N Zn) by vacuum induction melting. As-cast disks of ∅ 20 mm of these alloys obtained after grinding, sawing and chemical etching were first homogenized at 500°C during 5 h and then subjected to HPT at room temperature under the pressure of 6 GPa. The processing was carried out with the new modified HPT equipment with increased load capacity up to 2 MN [12,15] that enables to process metallic disc samples with the diameter up to 20 mm and a thickness of 0.8 mm. After HPT of the homogenized samples, the central (low-deformed) part of each disk (about 5 mm in diameter) was excluded from further investigations [15]. The samples for structural investigations were cut from the HPT-processed disks at a distance of 5 mm from the sample centre. TEM investigations have been carried out in a JEOL-2000EX microscope at an accelerating voltage of 120 kV. X-ray phase analysis was performed using a Pan Analytical X'Pert (Philips) diffractometer in Bragg-Brentano geometry with Cu Ka radiation and a position-sensitive detector (Philips X'Cellerator). The peak profiles fitted by the Profit (Philips) software were used for lattice parameter estimation. The mechanical tensile tests at room temperature were performed at the strain rates of 10^{-4} to 10^{-2} s^{-1}. The testing conditions (temperature, strain rate, load) were controlled by the computer software with accuracy of 2-3 %. The strength characteristics (yield strength $\sigma_{0.2}$ and ultimate strength σ_B) and ductility (relative elongation to failure δ) were determined from the results of the tests of non less than three samples with gage part dimensions of 1.2 x 1.0 x 0.4 mm.

Results and Discussions

The Al 6061 alloy. Observations by TEM showed that mainly subgrain structure of a lamellar type with clear orientation to shear plane was formed after ECAP-PC thorough one pass at 100°C (Fig. 2a). The mean cross subgrain size comprised 400 nm and longitudinal one made up 1200 nm correspondingly. Electron diffraction patterns prove subgrain structure formation with mainly low-angle grain boundary misorientaions (Fig. 2b).

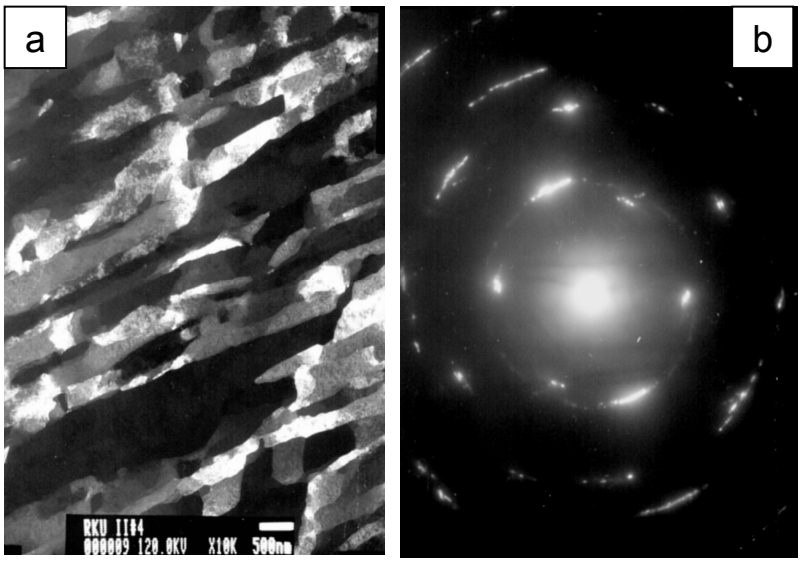

Fig. 2. Microstructure of Al 6061 alloy after ECAP-PC through one pass: dark field (a), SAED pattern (b).

After ECAP-PC through the second pass at the same temperature the structure changed significantly (Fig. 3). Fragmentation by means of cross-subboundary formation can be seen in elongated subgrains formed after ECAP-PC through 1 pass (Fig. 3 a,b). The electron diffraction patterns of

these areas are similar to that received after 1 ECAP pass and testify also to subgrain structure formation with mostly low-angle grain boundary misorientations (Fig. 3c). Separate areas (with a volume fraction of around ~ 30 %) of equi-axed grains of about 500 nm in size are observed as well in the structure along with subgrain fragmentation (Fig. 3 d,e).

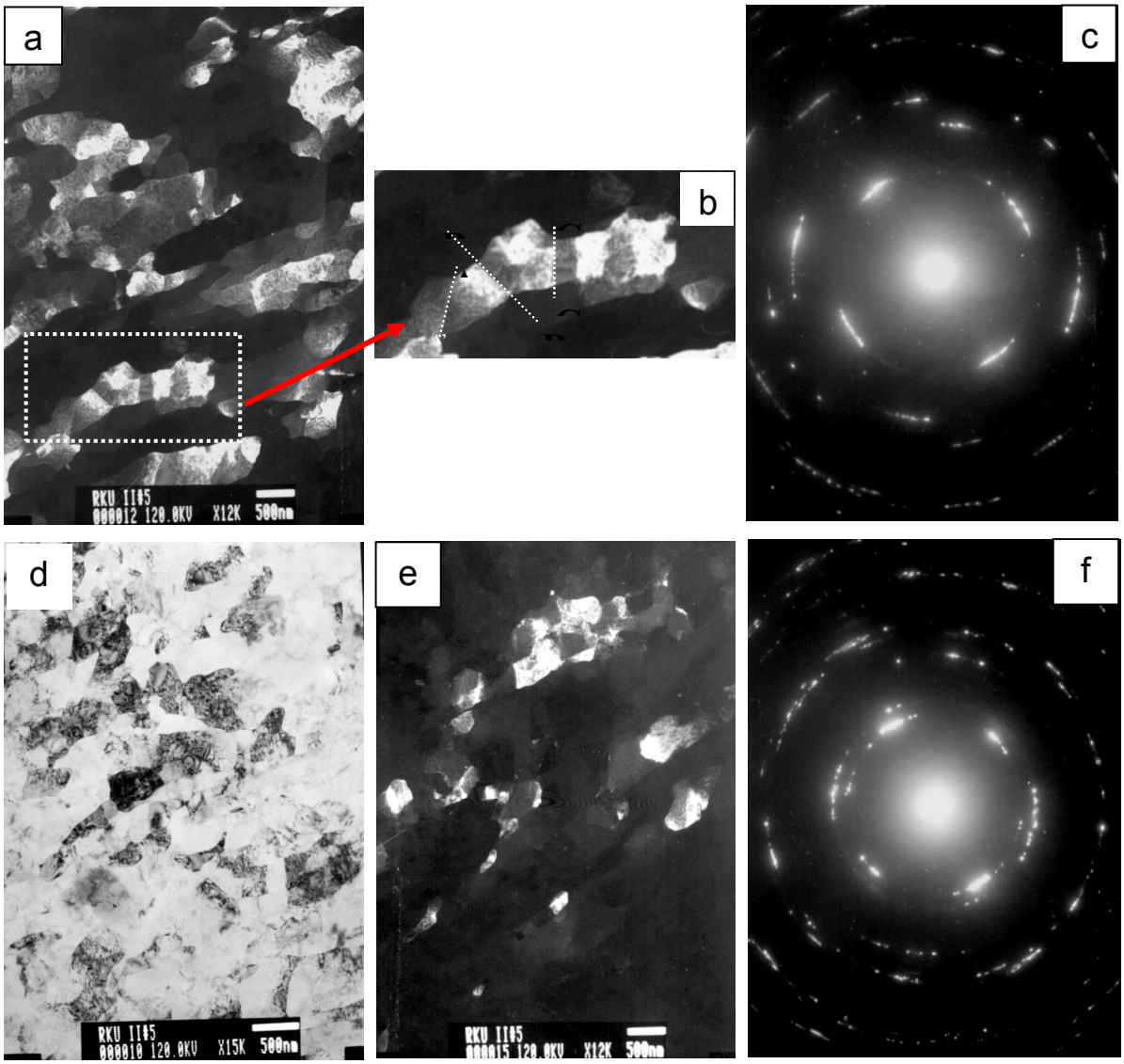

Fig. 3. Microstructure of the alloy after ECAP-PC through 2 passes: subgrain fragmentation (a, b), grain structure (d, e –bright and dark fields) SAED patterns (c, f).

The electron diffraction pattern (Fig. 3f) represents numerous spots distributed uniformly over the circles. This evidences of the formation of the UFG structure of a granular type with mostly high-angle grain boundaries at the areas.

The UFG structure formed after ECAP-PC through 4 passes is also of granular type in the longitudinal section (Fig. 4 a,b) as well as in the cross-section of the sample (Fig. 4 d). The electron diffraction pattern testifies to the granular structure with mainly high-angle grain boundary misorientations (Fig. 4 c). Besides, secondary phase dispersive precipitates of less than 10 nm in size were found in the alloy UFG structure after ECAP-PC (Fig. 4, A and B areas). According to the results [16,17] dealing with 6061 Al alloy processing by conventional ECAP, these dispersive precipitates represent Mg_2Si particles. These precipitates testify to the UFG structure formation being accompanied by dynamic aging at ECAP-PC through 4 passes. As the precipitates were not

found after the ECAP-PC through 1 and 2 passes, we can suggest that they are absent in these states, or their size was quite small and required investigations by high-resolution electron microscopy. It should be also noted that there were more lattice dislocations in the structure after 1 and/or 2 passes (Fig. 2 and 3) when compared to the structure formed in the material after 4 passes (Fig. 4).

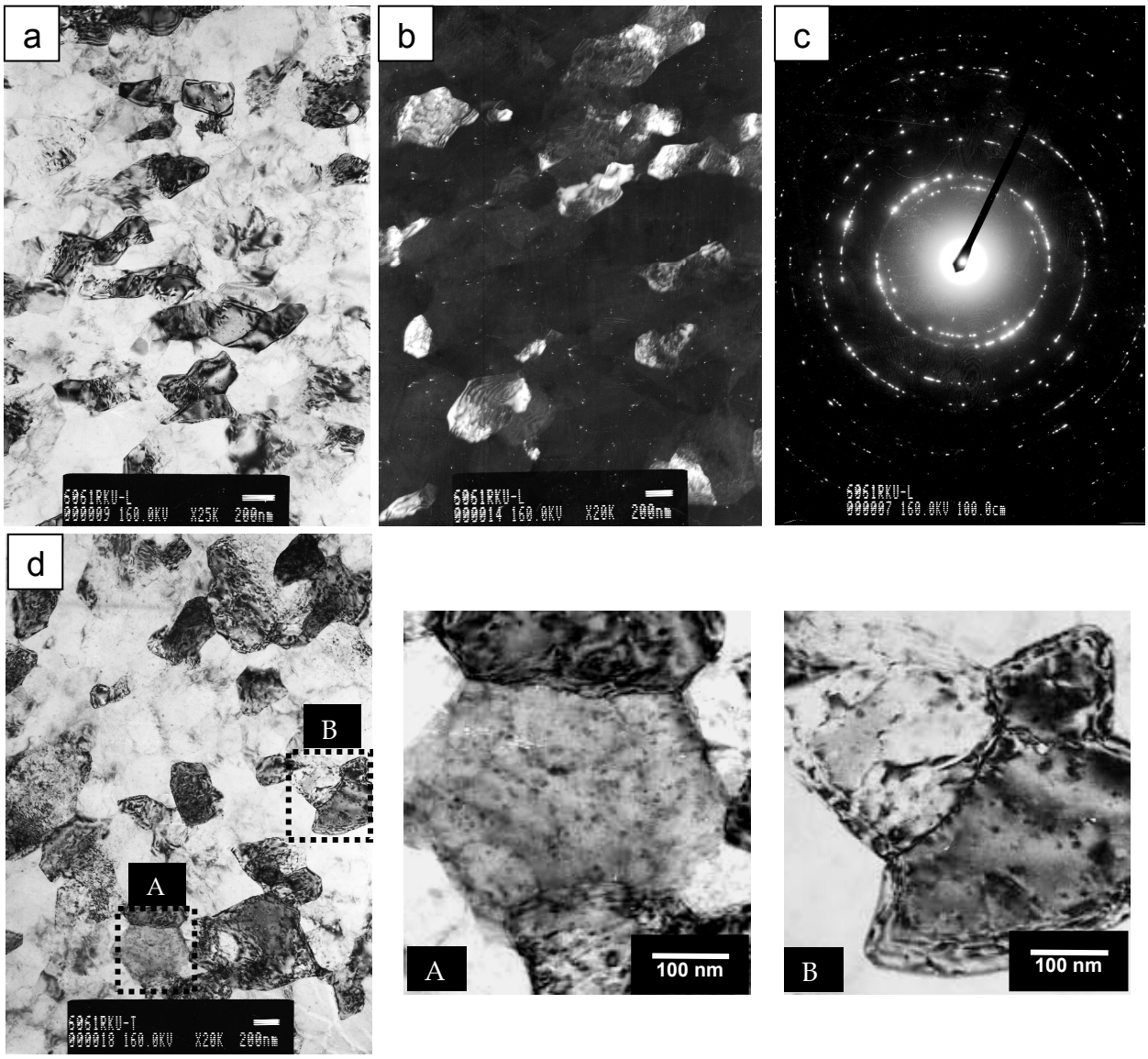

Fig. 4. Microstructure of the alloy after ECAP-PC through 4 passes in the longitudinal section of the sample (a,b), in the cross-section of the sample (disperse particles of Mg_2Si phase precipitated during the processing -areas A and B) (d), SAED pattern (c).

Mechanical properties of 6061 alloy after ECAP-PC through 1, 2 and 4 passes are presented in Fig. 5 and Table 1. The data can be compared with that of the same alloy after conventional T6 treatment (quenching at 535°C and subsequent artificial aging at 160°C for 12 hours).

The results correlate closely to the evolution of the microstructure revealed (Fig. 2-4). The formed substructure (Fig. 2) with a high density of lattice dislocations provides significant increase in strength after ECAP-PC through 1 pass, but its ductility is low enough and elongation to failure comprised ~ 6.5 %. The formation of the UFG structure of a combined type containing grains and subgrains (Fig. 3) in the billets after ECAP-PC through 2 passes provides some increase in both strength and ductility up to ~ 8 % (Table 1). At the same time the homogeneous UFG structure (Fig. 4) formed after ECAP-PC through 4 passes leads to insignificant loss in strength. However, its

ductility increases by two times and its elongation reaches ~ 20 %. Herewith, the UFG alloy demonstrates considerable uniform elongation which makes up ~ 9 %. Such a high value, which comprises ~ 40–45 % from total elongation, shows that the alloy with UFG structure has a potential to display enhanced fatigue [6,18].

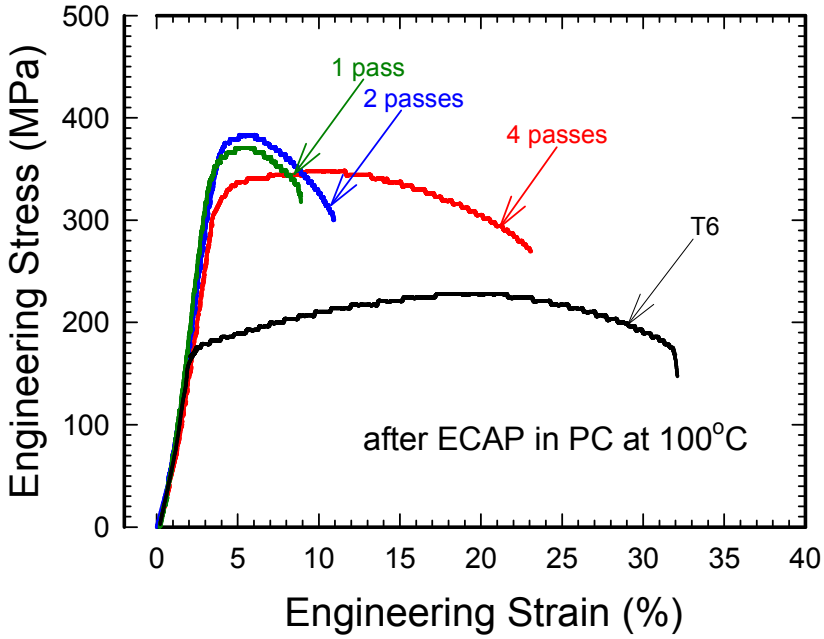

Fig. 5. The engineering stress-strain curves of the 6061 Al alloy at room temperature after ECAP-PC processing and convention heat-treatment (T6).

Treatment	UTS, MPa	YS, MPa	El., %
ECAP-PC at 100°C, 1 pass	370	335	6.5
ECAP-PC at 100°C, 2 passes	380	350	8.0
ECAP-PC at 100°C, 4 passes	345	305	20.0
T6	230	178	30.0

Table 1: Mechanical properties of the 6061 Al alloy at room temperature after ECAP-PC at 100°C.

Thus, the analysis of structural changes in the alloy 6061 after ECAP-PC at 100° C proves that the ECAP-PC technique makes it possible to produce a homogeneous UFG structure in a cast alloy after 4 passes in comparison with 8-10 passes in conventional ECAP [6,16], in other words, using of ECAP-PC can decrease the number of passes in 2-3 times under nearly the same processing conditions. Another advantage of the pressing is significant increase in the volume of UFG structure in a billet processed: about 85-90 % compared to 50-60 % after conventional ECAP. This can be of special interest for the process industrial application.

Regarding UFG structure formation in the alloy, an important feature of ECAP-PC is producing of practically equiaxed UFG structure already after 2 passes (Fig. 3), though the grains observed after the first pass were of elongated laminar structure (Fig. 2a). Gradual transformation of the grains to equiaxed ones is typical also of conventional ECAP [16]. At the same time, the present work proves the connection of this transformation with the formation of low-angle subgrain boundaries inside the elongated grains (Fig. 3a) and their following arrangement to high angle boundaries of the equiaxed UFG structure. Similar evolution of nanostructure during SPD processing has been discussed elsewhere [19].

One more effect revealed in the alloy after 4 passes is the formation of highly-disperse precipitations of the second phase, obviously, the particle of Mg_2Si phase. The formation of such particles evidences dynamic aging, which was observed recently in 6061 alloy after conventional ECAP [16,17]. However, this time the aging occurs at a low temperature (100°C) and ageing time less than 10 minutes, which is considerably lower, than 175°C, 8 hours of the peak aging condition (T6) for a 6061 alloy [16]. Such an acceleration of aging kinetics can result from high vacancy concentration during processing. Recent "in situ" HPT experiments in synchrotron beamline showed [20] that excess vacancy concentration can reach 10^{-5}, which is near to equilibrium concentration at melting temperature point. Besides, 3D atom probe applied to the alloy showed the formation of alloying elements segregations after HPT even at room temperature [21]. Such segregations appear to be the second phase precipitations at the subsequent deformation. Thus, aging processes are more rapid at ECAP-PC, which can influence the alloy's mechanical behavior.

It is well-known, that ECAP-PC processing significantly increases the strength, but reduces ductility. The Al 6061 alloy after ECAP-PC through 1 and 2 passes behaved in accordance with this rule. However, it showed considerable increase in ductility with the small reduction of strength (to 30-40 MPa) after ECAP-PC through 4 passes. Such extraordinary combination of high strength and high ductility of UFG Al alloy was also observed recently [8,22-24]. This attractive mechanical behavior can be caused by either formation of UFG structure with high-angle grain boundaries capable to grain boundary sliding [23], or difficulty in strain localization due to the presence of disperse particles [8]. We are planning to study the phenomenon in detail in our ongoing research.

The Al-30%Zn alloy. The microstructure after HPT contains equiaxial ultrafine Al grains with the size about 380 nm (see TEM micrograph in Fig. 6a). Smaller (50 to 150 nm) Zn grains are located in the triple junctions of Al GBs (Fig. 6b) [15]. Slight amount of very fine Zn grains (grain size of 5 to 15 nm) is also present inside the Al-grains. XRD peaks of Al revealed rather low microstrain contribution into peak broadening. The analysis of Al peak broadening proved the microstrain level of 0.010 ± 0.002 %. XRD also allowed estimating the dislocation density of about 10^{12} m^{-2}. This value correlates well with TEM data showing that the Al-grains are almost free from the lattice dislocations (Fig. 6). The evolution of microstructure of the studied alloy correlates with its microhardness. It is 970 MPa in the as-cast state and increased up to 1670 MPA after homogenization and quenching. This increase was driven by the formation of the supersaturated Zn-rich Al-based solid solution. HPT resulted in the drastic softening of the samples down to 490 MPa due to the full decomposition of the Zn-reach Al-based solid solution during HPT. Similar HPT-driven softening was already observed in the as-cast Al–Zn alloys [14].

The obtained dependences of flow stress, σ_{max}, on the elongation to failure, δ, for various strain rates, $\dot{\varepsilon}$, are shown in Fig. 7a. The dependence of flow stress, σ, on the strain rate, $\dot{\varepsilon}$, is shown in Fig. 7b. The values of strain rate sensitivity, m, are also given in Fig. 7b. The studied HPT-deformed ultrafine-grained Al alloy demonstrates the ductility which is unusually high for the room temperature. The maximal elongation-to-failure of about 160 % was reached by $\dot{\varepsilon} = 10^{-4}$ s^{-1}. The value $\sigma_{max}(\dot{\varepsilon})$ increases monotonically with increasing $\dot{\varepsilon}$. The strain rate sensitivity observed for $\dot{\varepsilon}$ between 10^{-3} s^{-1} and 10^{-4} s^{-1} is extremely high: m = 0.24 to 0.29. Such m values are close to ones typical for the superplastic behavior and were usually observed only at high temperatures above 0.5 T_m (T_m being the melting temperature) [25]. The observed δ and m values reveal that the studied

material becomes superductile at room temperature. Such behavior was never observed before in the Al-based alloys at room temperature.

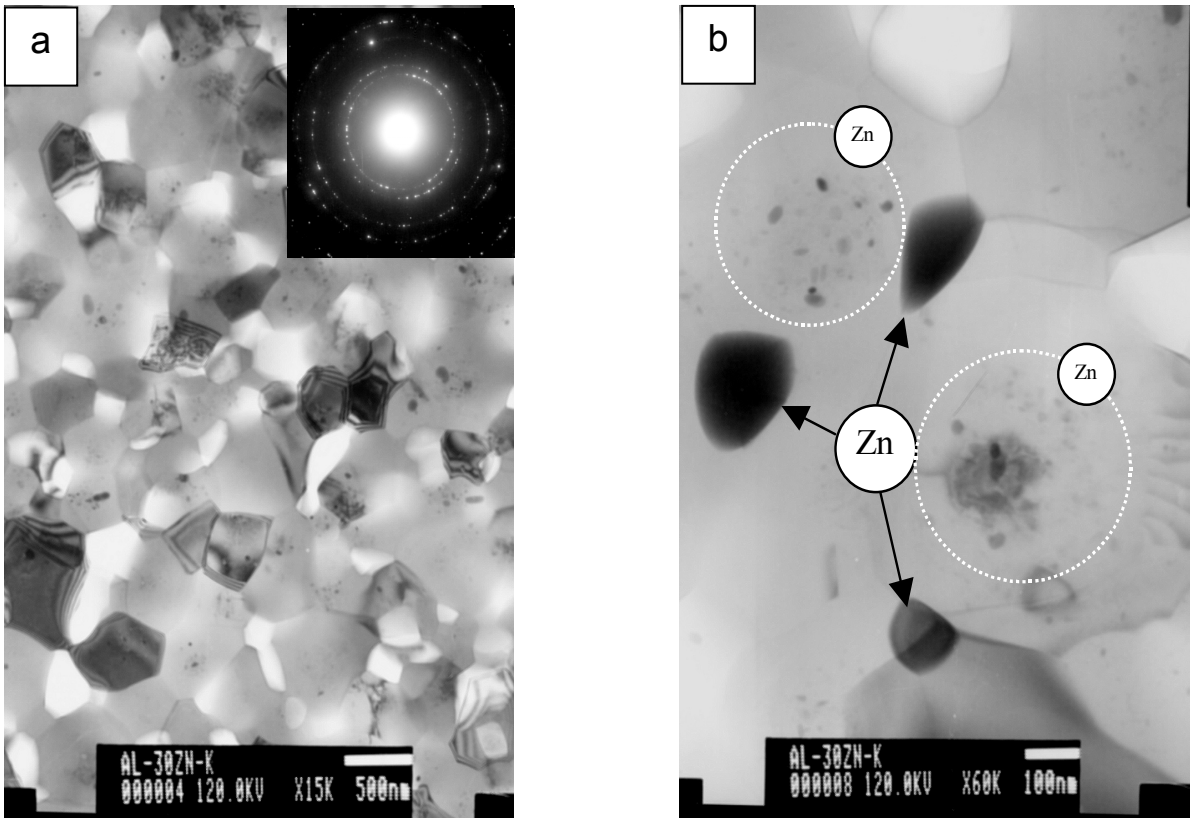

Fig. 6. Microstructure of the Al-30Zn alloy formed in the billet processed by HPT (a), and Zn-phase precipitations at triple junction and inside the Al grains (b).

Why does the studied UFG Al–Zn alloy become super-ductile at ambient temperature, and other Al-based alloys (including pure Al) do not? We suppose that the reason for this phenomenon is appearance of the thin layers of the Zn-rich grain boundary phase resulting in enhanced GB sliding. Thus, the state with high ductility can correspond to the UFG structure with high amount of (Al)/(Al) GBs wetted (covered) by Zn layers. This structure results from the so-called GB wetting phase transition. GB wetting phase transformation proceeds at the temperature T_{wGB} where GB energy in σ_{GB} becomes higher than the energy of two solid/liquid interfaces $2\sigma_{SL}$ or two solid/solid interfaces $2\sigma_{SS}$ [26-29]. From the bulk Al–Zn phase diagram it appears that the Al–Zn system belongs to the "classical" Cahn's systems with a critical point for a binary solution [26,30-32]. Both GB wetting by solid and liquid phases is possible in the Al–Zn system due to the rather low energy of Al/Zn interfaces [33,34]. In other words, all Al/Al GBs at room temperature have to be covered by a layer of Zn. This layer may be rather thin depending on the Zn content and the time for equilibration. Moreover, during SPD processing leading to formation of ultrafine grains vacancy concentration and diffusion coefficient increase by 4-5 times and GB energy grows considerably (by 70-80%) due to the appearance of excess defect density [20], which also contributes to the formation of thin boundary Zn layer in the UFG Al–30 wt. % Zn alloy, "lubricating" GBs. It is not easy to observe the thin GB films [29,32], and our separate future work will be devoted to their structural observation.

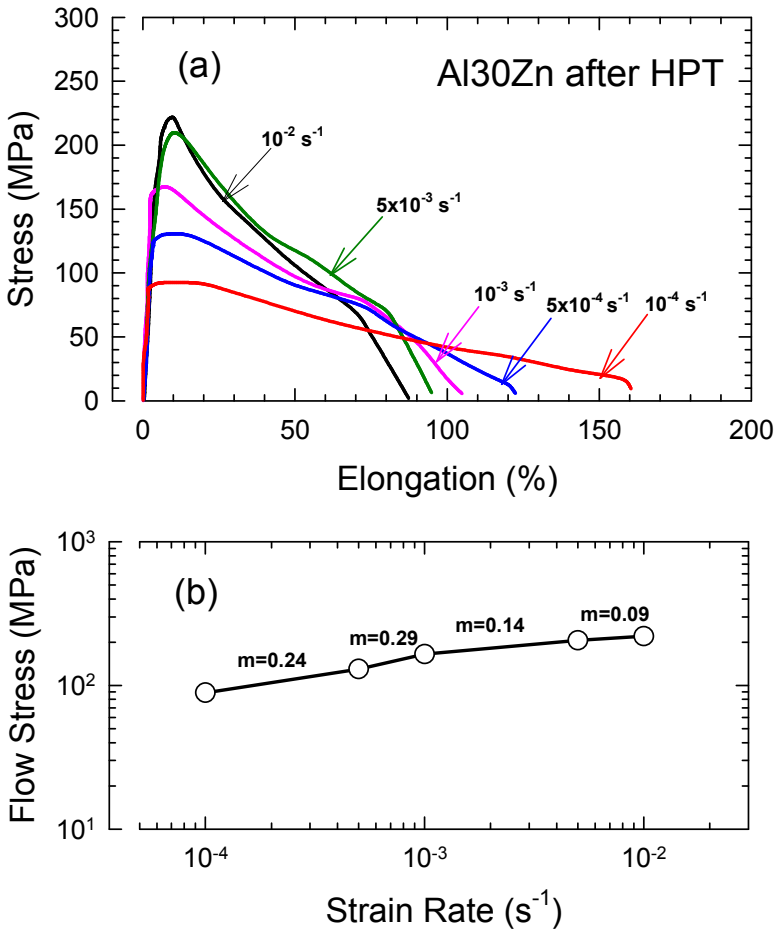

Fig. 7. Effect of strain rate on the true stress-strain curves (a) and the variation of flow stress and strain rate sensitivity coefficient, *m*, with strain rate (b) for the HPT processed Al-30Zn alloy.

The idea of the "lubricating" Zn GB layers in Al-alloys is supported also by the estimations of GB sliding input into total ductility. GB sliding is known to be the deformation mechanism which is typically responsible for the enhanced strain rate sensitivity and leads, in turn, to the structural superplasticity in fine-grained materials. The constitutive relationship for grain boundary sliding can be written as [25]:

$$\dot{\varepsilon} = A\,(D/kT)\,(\sigma/G)^n\,(b/d)^p, \qquad (1)$$

where $\dot{\varepsilon}$ is the strain rate, D is the appropriate temperature dependent diffusivity, A is a dimensionless mechanism-dependent constant, G is the shear modulus, b is the Burgers vector, $n = m^{-1}$ is the stress exponent, and p is the grain size exponent for the given grain size d.

Unlike most superplastic materials, where strain rate sensitivity m is around 0.5 and observed at elevated temperatures ($\geq 0.5\ T_m$), the m value for the studied superductile Al–30 wt. % Zn alloy is only 0.24 for elongation of 160%. In this case the apparent stress exponent is not $n = 2$ (as typically), but $n = 4$. Substituting further $\sigma = 100$ MPa, $\dot{\varepsilon} = 2.5\times10^{-4}$ s^{-1}, $d = 380$ nm, $p = 2$ and $A = 1.5\times10^{-3}$ [35] into equation (1), an agreement with experimental data is achieved for $D = 7\times10^{-16}$ m^{-2}s^{-1}. The value of D indicates, that some kind of diffusion process controls the steady-state deformation (i.e. bulk or GB diffusion).

What does it mean that $D = 7\times10^{-16}$ m^{-2}s^{-1} in our case, i.e. which process controls the ductile behaviour of the UFG Al–30 wt. % Zn alloy at room temperature? The extrapolation of bulk values to 300K gives for self-diffusion in Al $D = 10^{-29}$ m^{-2}s^{-1}, for Zn diffusion in Al $D = 10^{-24}$ m^{-2}s^{-1} and

self-diffusion in Zn $D = 10^{-21}$ $m^{-2}s^{-1}$ [36]. These values permit to completely exclude the bulk diffusion as possible mechanism for the observed plastic behaviour. In case of GB diffusion, the extrapolation of Al self-diffusion along Al/Al GBs to room temperature gives the value of $D_b = 10^{-19}$ $m^{-2}s^{-1}$ [36,37]. However D_b (Zn) measured along Al/Al GBs at room temperature is about $D_b = 10^{-15}$ $m^{-2}s^{-1}$ [36,37]. These data excellently correlate with D estimation from Eq. (1). It means that the observed superductile behaviour at room temperature in the UFG Al–30 wt. % Zn alloy is controlled by the GB sliding and Zn diffusion along the Al/Al GBs. The diffusion coefficient of Zn along Zn/Zn GBs at 300K is about $D_b = 10^{-13}$ $m^{-2}s^{-1}$ [36,37]. It means that if Zn completely wets the Al GBs during grain refinement by SPD processing, the Zn layer would "lubricate" GB providing easier GB sliding and enhancing ductility. This idea permits us to propose the way, how to reach the combination of high strength and ductility using the GB wetting transitions in ultrafine-grained alloys. The high strength would be ensured by the ultrafine matrix grains of component A with high melting temperature. The high ductility would be ensured by the thin equilibrium wetting layers of component B with lower melting temperature along A/A grains.

Conclusions

Thus, in the present paper we successfully demonstrated the possibility to enhance ductility of UFG Al alloys through GB engineering by modification of two SPD techniques, namely ECAP-PC and HPT with increased load. The data obtained show that the formation of high-angle grain boundaries and enhanced GB diffusion provide conditions for GB sliding and might be efficiently used for the control of mechanical properties of UFG Al alloys. However, the concept of GB engineering calls for further investigations aimed at its development and in the first place, establishment of GB atomic structure features in SPD-processed materials and their behavior in deformation processes.

Acknowledgements

The present paper was supported in part through grants of the Ministry for Education and Science of the Russian Federation and Russian Foundation for Basic Research as well as by the NIS-IPP Program of DOE (USA). Cooperation with co-authors mentioned in references is gratefully acknowledged as well.

References

[1] R.Z. Valiev, R.K. Islamgaliev, I.V. Alexandrov: Prog. Mater. Sci. Vol. 45 (2000), p. 103

[2] M.J. Zehetbauer (Ed.): Adv Eng Mater, Special Issue on Nanomaterials by Severe Plastic Deformation, Vol. 5 (2003).

[3] Z. Horita (Ed.) *Proc. 3rd Int. Conf. on Nanomaterials by Severe Plastic Deformation,* (Trans Tech Publications LTD, Switzerland, 2006).

[4] R.Z. Valiev, Yu. Estrin, Z. Horita, T.G. Langdon, M.J. Zehetbauer and Y.T. Zhu: JOM Vol. 58 No. 4 (2006), p. 33

[5] R.Z. Valiev, A.V. Korznikov and R.R. Mulyukov: Mater. Sci. Eng. A Vol. 168, No. 2 (1993), p. 141

[6] R.Z. Valiev, T.G. Langdon: Prog. Mater. Sci. Vol. 51 (2006), p. 881

[7] E. Ma: JOM Vol. 58, No. 4 (2006), p. 49

[8] Z. Horita, K. Ohashi, T. Fujita, K. Kaneko, T.G. Langdon: Adv. Mater. Vol. 17 (2005), p. 1599

[9] R.Z. Valiev: Nature Mater. Vol. 3 (2004), p. 511

[10] R.Z. Valiev: Mater. Sci. Forum Vols. 584—586 (2008), p. 22

[11] G.I. Raab: Mater Sci Eng A Vols. 410-411 (2005), p. 230

[12] M. Yu. Murashkin, A.R. Kilmametov, and R.Z. Valiev: Phys. Metal. Metallogr. Vol. 106, No. 1, (2008), p. 90

[13] J.R. Davis (ed): *ASM Special Handbook. Aluminium and Aluminium Alloys* (1993).

[14] A.A. Mazilkin, B.B. Straumal, E. Rabkin, B. Baretzky, S. Enders, S.G. Protasova, O.A. Kogtenkova, and R.Z. Valiev: Acta Mater. Vol. 54, (2006), p. 3933

[15] R.Z. Valiev, M.Yu. Murashkin, A.R. Kilmametov, B.B. Straumal: to be submitted.

[16] W.J. Kim, J.K. Kim, T.Y. Park, S.I. Hong, D.I. Kim, Y.S. Kim and J.D. Lee: Metall. Mater. Trans. Vol. 33A (2002), p. 3155

[17] G. Nurislamova, X. Sauvage, M. Murashkin, R. Valiev: in Ultrafine Grained Materials IV. ed. By Y.T. Zhu, T.G. Langdon, Z. Horita *et al.* TMS 2006 Annual Meeting in San Antonio, Texas, USA March 12-16, 2006. pp. 41-45

[18] A.Yu. Vinogradov, V.V. Stolyarov, S. Hashimoto, R.Z. Valiev: Mater. Sci. Eng. A Vol. 318 (2001) p. 163

[19] R.Z. Valiev, Yu.V. Ivanisenko, E.F. Rauch and B. Baudelet: Acta Mater. Vol. 44 (1996), p. 4705.

[20] A.R. Kilmametov, G. Vaughan, A. R. Yavari, A. LeMoulec, W.J. Botta and R. Z. Valiev: Mater. Sci. Eng. A Vol. 503 (2009), p. 10

[21] G. Nurislamova, X. Sauvage, M. Murashkin, R. Islamgaliev, R. Valiev: Phil. Mag. Lett. Vol. 88 (2008), p. 459.

[22] H.J. Roven, H. Nesboe, J.C. Werenskiold, T. Seibert: Mater. Sci. Eng. A Vols. 410–411 (2005), p. 426

[23] I. Sabirov, Y. Estrin, M.R. Barnett, I. Timokhina, P.D. Hodson: Acta Mater. Vol. 56 (2008), p. 2223

[24] R.Z. Valiev, M.Yu. Murashkin, E.V. Bobruk, and G.I. Raab: Mater. Trans. Vol. 50, No. 1 (2009), p 87

[25] T.G. Langdon: J. Mater. Sci. Vol. 41 (2006), p. 597

[26] J.W. Cahn: J. Chem. Phys. Vol. 66 (1977), p. 3667

[27] B.B. Straumal, O. Kogtenkova, and P. Zięba: Acta Mater. Vol. 56, (2008), p. 925

[28] B.B. Straumal: *Grain boundary phase transitions* (Moscow: Nauka publishers, 2003), in Russian.

[29] B.B. Straumal, A.A. Mazilkin, O.A. Kogtenkova, S.G. Protasova, and B. Baretzky: Phil. Mag. Lett. Vol. 87, (2007), p. 423

[30] B.B. Straumal, A.S. Gornakova, O.A. Kogtenkova, S.G. Protasova, V.G. Sursaeva, and B. Baretzky: Phys. Rev. B Vol. 78 (2008), p. 054202

[31] T.B. Massalski (ed.) (1990) *Binary Alloy Phase Diagrams,* 2nd ed. ASM International, Materials Park, OH, pp. 238–242.

[32] B. Straumal, R. Valiev, O. Kogtenkova, P. Zieba, T. Czeppe, E. Bielanska, and M. Faryna: Acta Mater. Vol. 56 (2008), p. 6123

[33] Y.J. Gao, Y.J. Han: Mater. Sci. Forum. Vols. 475-479 (2005), p. 3131

[34] B.B. Straumal, O.A. Kogtenkova, S.G. Protasova, A.N. Nekrasov, B. Baretzky: JETP Letters (2009) in press.

[35] R.Z. Valiev, E.V. Kozlov, Yu.F. Ivanov, J. Lian, A.A. Nazarov, and B. Baudelet: Acta Metall. Mater. Vol. 42 (1994), p. 2467

[36] H. Mehrer (ed.): *Diffusion in Solid Metals and Alloys. Landolt-Börnstein*, Vol. 26 (Springer, Berlin etc., 1990).

[37] I. Kaur, W. Gust, L. Kosma: *Handbook of interphase and grain boundary diffusion* (Ziegler press, Stuttgart, 1989).

Ductility of Bulk Nanostructured Materials
doi:10.4028/www.scientific.net/MSF.633-634

Enhanced Ductility in Ultrafine-Grained Al Alloys Produced by SPD Techniques
doi:10.4028/www.scientific.net/MSF.633-634.321

References

[1] R.Z. Valiev, R.K. Islamgaliev, I.V. Alexandrov: Prog. Mater. Sci. Vol. 45 (2000), p. 103
doi:10.1016/S0079-6425(99)00007-9

[2] M.J. Zehetbauer (Ed.): Adv Eng Mater, Special Issue on Nanomaterials by Severe Plastic Deformation, Vol. 5 (2003).

[3] Z. Horita (Ed.) Proc. 3rd Int. Conf. on Nanomaterials by Severe Plastic Deformation, (Trans Tech Publications LTD, Switzerland, 2006).

[4] R.Z. Valiev, Yu. Estrin, Z. Horita, T.G. Langdon, M.J. Zehetbauer and Y.T. Zhu: JOM Vol. 58 No. 4 (2006), p. 33
doi:10.1007/s11837-006-0213-7

[5] R.Z. Valiev, A.V. Korznikov and R.R. Mulyukov: Mater. Sci. Eng. A Vol. 168, No. 2 (1993), p. 141
doi:10.1016/0921-5093(93)90717-S

[6] R.Z. Valiev, T.G. Langdon: Prog. Mater. Sci. Vol. 51 (2006), p. 881
doi:10.1016/j.pmatsci.2006.02.003

[7] E. Ma: JOM Vol. 58, No. 4 (2006), p. 49
doi:10.1007/s11837-006-0215-5

[8] Z. Horita, K. Ohashi, T. Fujita, K. Kaneko, T.G. Langdon: Adv. Mater. Vol. 17 (2005), p. 1599
doi:10.1002/adma.200500069

[9] R.Z. Valiev: Nature Mater. Vol. 3 (2004), p. 511
doi:10.1038/nmat1180

[10] R.Z. Valiev: Mater. Sci. Forum Vols. 584—586 (2008), p. 22
doi:10.4028/www.scientific.net/MSF.584-586.22

[11] G.I. Raab: Mater Sci Eng A Vols. 410-411 (2005), p. 230
doi:10.1016/j.msea.2005.08.089

[12] M. Yu. Murashkin, A.R. Kilmametov, and R.Z. Valiev: Phys. Metal. Metallogr. Vol. 106, No. 1, (2008), p. 90
doi:10.1134/S0031918X08070120

[13] J.R. Davis (ed): ASM Special Handbook. Aluminium and Aluminium Alloys (1993).

[14] A.A. Mazilkin, B.B. Straumal, E. Rabkin, B. Baretzky, S. Enders, S.G. Protasova, O.A. Kogtenkova, and R.Z. Valiev: Acta Mater. Vol. 54, (2006), p. 3933
doi:10.1016/j.actamat.2006.04.025

[15] R.Z. Valiev, M.Yu. Murashkin, A.R. Kilmametov, B.B. Straumal: to be submitted.

[16] W.J. Kim, J.K. Kim, T.Y. Park, S.I. Hong, D.I. Kim, Y.S. Kim and J.D. Lee: Metall. Mater. Trans. Vol. 33A (2002), p. 3155
doi:10.1007/s11661-002-0301-4

[17] G. Nurislamova, X. Sauvage, M. Murashkin, R. Valiev: in Ultrafine Grained Materials IV. ed. By Y.T. Zhu, T.G. Langdon, Z. Horita et al. TMS 2006 Annual Meeting in San Antonio, Texas, USA March 12-16, 2006. pp. 41-45

[18] A.Yu. Vinogradov, V.V. Stolyarov, S. Hashimoto, R.Z. Valiev: Mater. Sci. Eng. A Vol. 318 (2001) p. 163
doi:10.1016/S0921-5093(01)01262-X

[19] R.Z. Valiev, Yu.V. Ivanisenko, E.F. Rauch and B. Baudelet: Acta Mater. Vol. 44 (1996), p. 4705.
doi:10.1016/S1359-6454(96)00156-5

[20] A.R. Kilmametov, G. Vaughan, A. R. Yavari, A. LeMoulec, W.J. Botta and R. Z. Valiev: Mater. Sci. Eng. A Vol. 503 (2009), p. 10
doi:10.1016/j.msea.2008.11.023

[21] G. Nurislamova, X. Sauvage, M. Murashkin, R. Islamgaliev, R. Valiev: Phil. Mag. Lett. Vol. 88 (2008), p. 459.
doi:10.1080/09500830802186938

[22] H.J. Roven, H. Nesboe, J.C. Werenskiold, T. Seibert: Mater. Sci. Eng. A Vols. 410–411 (2005), p. 426
doi:10.1016/j.msea.2005.08.112

[23] I. Sabirov, Y. Estrin, M.R. Barnett, I. Timokhina, P.D. Hodson: Acta Mater. Vol. 56 (2008), p. 2223
doi:10.1016/j.actamat.2008.01.020

[24] R.Z. Valiev, M.Yu. Murashkin, E.V. Bobruk, and G.I. Raab: Mater. Trans. Vol. 50, No. 1 (2009), p 87

doi:10.2320/matertrans.MD200821

[25] T.G. Langdon: J. Mater. Sci. Vol. 41 (2006), p. 597
doi:10.1007/s10853-006-6476-0

[26] J.W. Cahn: J. Chem. Phys. Vol. 66 (1977), p. 3667
doi:10.1063/1.434402

[27] B.B. Straumal, O. Kogtenkova, and P. Ziba: Acta Mater. Vol. 56, (2008), p. 925
doi:10.1016/j.actamat.2007.10.043

[28] B.B. Straumal: Grain boundary phase transitions (Moscow: Nauka publishers, 2003), in Russian.

[29] B.B. Straumal, A.A. Mazilkin, O.A. Kogtenkova, S.G. Protasova, and B. Baretzky: Phil. Mag. Lett. Vol. 87, (2007), p. 423
doi:10.1080/09500830701225787

[30] B.B. Straumal, A.S. Gornakova, O.A. Kogtenkova, S.G. Protasova, V.G. Sursaeva, and B. Baretzky: Phys. Rev. B Vol. 78 (2008), p. 054202
doi:10.1103/PhysRevB.78.054202

[31] T.B. Massalski (ed.) (1990) Binary Alloy Phase Diagrams, 2nd ed. ASM International, Materials Park, OH, pp. 238–242.

[32] B. Straumal, R. Valiev, O. Kogtenkova, P. Zieba, T. Czeppe, E. Bielanska, and M. Faryna: Acta Mater. Vol. 56 (2008), p. 6123
doi:10.1016/j.actamat.2008.08.021

[33] Y.J. Gao, Y.J. Han: Mater. Sci. Forum. Vols. 475-479 (2005), p. 3131
doi:10.4028/www.scientific.net/MSF.475-479.3131

[34] B.B. Straumal, O.A. Kogtenkova, S.G. Protasova, A.N. Nekrasov, B. Baretzky: JETP Letters (2009) in press.

[35] R.Z. Valiev, E.V. Kozlov, Yu.F. Ivanov, J. Lian, A.A. Nazarov, and B. Baudelet: Acta Metall. Mater. Vol. 42 (1994), p. 2467
doi:10.1016/0956-7151(94)90326-3

[36] H. Mehrer (ed.): Diffusion in Solid Metals and Alloys. Landolt-Börnstein, Vol. 26 (Springer, Berlin etc., 1990).

[37] I. Kaur, W. Gust, L. Kosma: Handbook of interphase and grain boundary diffusion (Ziegler press, Stuttgart, 1989).